MOLECULAR AND CELLULAR BIOLOGY, Sept. 2006, p. 6547–6556 Vol. 26, No. 17
0270-7306/06/$08.00+0 doi:10.1128/MCB.00284-06

dysfusion Transcriptional Control of *Drosophila* Tracheal Migration, Adhesion, and Fusion

Lan Jiang and Stephen T. Crews*

Department of Biochemistry and Biophysics and Department of Biology, Program in Molecular Biology and Biotechnology, The University of North Carolina at Chapel Hill, Chapel Hill, North Carolina 27599-3280

Received 15 February 2006/Returned for modification 24 April 2006/Accepted 7 June 2006

The *Drosophila dysfusion* basic-helix-loop-helix–PAS transcription factor gene is expressed in specialized fusion cells that reside at the tips of migrating tracheal branches. *dysfusion* mutants were isolated, and genetic analysis of live embryos revealed that mutant tracheal branches migrate to close proximity but fail to recognize and adhere to each other. Misexpression of *dysfusion* throughout the trachea further indicated that *dysfusion* has the ability to both inhibit cell migration and promote ectopic tracheal fusion. Nineteen genes whose expression either increases or decreases in fusion cells during development were analyzed in *dysfusion* mutant embryos. *dysfusion* upregulates the levels of four genes, including the *shotgun* cell adhesion protein gene and the zona pellucida family transmembrane protein gene, *CG13196*. Misexpression experiments with *CG13196* result in ectopic tracheal fusion events, suggesting that it also encodes a cell adhesion protein. Another target gene of *dysfusion* is *members only*, which inhibits protein nuclear export and influences tracheal fusion. *dysfusion* also indirectly downregulates protein levels of Trachealess, an important regulator of tracheal development. These results indicate that fusion cells undergo dynamic changes in gene expression as they switch from migratory to fusion modes and that *dysfusion* regulates a discrete, but important, set of these genes.

One important aspect of insect tracheal morphogenesis involves the fusion of tracheal branches to form an interconnected oxygen-bearing tubular network (8). Branches contain a specialized fusion cell at their tips (26). These fusion cells extend actin-rich filopodia (24, 31) that guide migration in response to guidance cues, similar to axonal growth cone guidance (6). Thus, tracheal branches from adjacent hemisegments are directed to close proximity by the external guidance cues and then recognize and adhere to each other. After joining, further cellular changes occur, including (i) cytoskeletal reorganization, (ii) the breaking and reassembling of cellular junctions, and (iii) the formation of a continuous lumen (34). The complexity of tracheal branching and fusion suggests that the fusion cell is a complex, dynamic structure with changing patterns of gene expression. One of the major challenges in studying tracheal morphogenesis is to understand how regulatory pathways control and coordinate these changes in gene expression.

The molecular biology, cell biology, and genetics of branch migration and fusion have been productively studied in recent years. The trachea-expressed Breathless (Btl) tyrosine kinase receptor is activated by Branchless and is required for filopodial extension and migration (14, 24, 30). Additional proteins, such as Roundabout (Robo), Robo2, and Slit, are involved in branch-specific pathfinding (6). Analysis of enhancer trap lines first led to the identification of genes prominently expressed in or absent from fusion cells (26), and their regulation was initiated with the discovery of the *escargot* (*esg*) gene (27, 31), which encodes a zinc finger transcription factor. *esg* is expressed specifically in fusion cells during branching, and *esg* mutants have defects in tracheal fusion. Several genes whose expression is dependent on *esg* were identified. They included *shotgun* (*shg*), whose levels are upregulated in fusion cells, and *Drosophila serum response factor* (*DSRF*), which is expressed in adjacent terminal tracheal cells but repressed in fusion cells. Shg, a cadherin cell surface protein, is implicated in adhesive interactions and the formation of new adherens junctions in the fused trachea (31, 33). These results and other discoveries began to dissect the cellular and molecular bases of tracheal branch migration and fusion.

Another transcriptional target of Esg is *dysfusion* (*dys*), which encodes a basic-helix-loop-helix–PAS (bHLH-PAS) transcription factor that is expressed specifically in all fusion cells (12). RNA interference (RNAi)-mediated reduction of *Drosophila dys* function demonstrated that the dorsal branches (DBs), lateral trunk (LT) branches, and ganglionic branches (GBs) failed to fuse, although the cellular and molecular natures of these defects were not assessed. Dys is evolutionarily well conserved with a human ortholog (*NXF* or *LE-PAS*) that is prominently expressed in the brain (17, 21) and with a *Caenorhabditis elegans* ortholog (*C15C8*.2) that is expressed in the pharynx (23). Particularly noteworthy is the existence of several other *Drosophila* bHLH-PAS proteins that have important roles in tracheal development. The *trachealess* (*trh*) gene plays an early role in initiating tracheagenesis (10, 37) and directly regulates *btl* (20). The *similar* (*sima*) gene encodes the *Drosophila* ortholog of mammalian hypoxia-inducible factors (19) and functions in trachea to control the transcriptional response to hypoxia (1, 4, 16). All three proteins function as heterodimers with the same bHLH-PAS protein, Tango (Tgo) (29). Interestingly, Trh levels in fusion cells are reduced as Dys appears, and the reduction is dependent on *dys* function (12). Several questions arise regarding the function of *dys*. At the

* Corresponding author. Mailing address: Department of Biochemistry and Biophysics and Department of Biology, Program in Molecular Biology and Biotechnology, The University of North Carolina at Chapel Hill, Chapel Hill, NC 27599-3280. Phone: (919) 962-4380. Fax: (919) 962-4296. E-mail: steve_crews@unc.edu.

cellular level, does Dys function in branch migration, cell recognition/adhesion, or fusion events? What genes are regulated by *dys*, and do they constitute a functionally discrete subset of *esg*-regulated genes? Do *dys*-regulated genes share common biochemical functions? Are Trh protein levels and other genes downregulated by *dys* via transcriptional, posttranscriptional, or competitive mechanisms? How widespread are transcriptional changes in fusion cells?

In this study, the dynamics of fusion cell gene expression were examined and the functional role of *dys* investigated in much greater detail than previously reported. *dys* mutants were isolated, and analysis of their phenotypes showed that branch migration is normal but fusion cells fail to stably adhere, resulting in a failure of tracheal fusion. Misexpression of *dys* throughout the trachea resulted in severely malformed trachea in which secondary and tertiary branching was stunted and lumen formation inhibited at fusion sites. In addition, misexpression embryos often showed ectopic fusion events. Nineteen trachea-expressed genes were analyzed in wild-type and *dys* mutant embryos. Levels of four fusion cell-expressed genes declined in *dys* mutants. Misexpression of *dys* also resulted in ectopic expression of target genes. Two target genes are implicated in tracheal cell adhesion: *shg* and *CG13196*, a zona pellucida (ZP) gene (11). Embryos that misexpress *CG13196* showed tracheal abnormalities consistent with it functioning as an adhesion protein gene. In addition, *dys* can indirectly regulate fusion cell protein levels and subcellular localization. Thus, *dys* controls multiple aspects of tracheal fusion, by upregulating and downregulating fusion cell constituents by using direct and indirect biochemical mechanisms.

MATERIALS AND METHODS

***Drosophila* strains.** The *Drosophila* strain *Df(3R)Espl3* [96F1; 97B1] is deleted for the *dys* gene and was utilized in an ethyl methanesulfonate (EMS) screen to obtain *dys* mutants. Additional deletion strains used to characterize the EMS-generated mutants were *Df(3R)Exel6204* [96F9; 97A6] and *Df(3R)ME61* [96F12-14; 97C4-5] (all three deficiency strains are available from the Bloomington *Drosophila* Stock Center). In addition, the EMS-generated mutants were crossed to gro^1, which is uncovered by *Df(3R)Espl3*. Misexpression experiments utilized *btl-Gal4* (Tien Hsu) (28), *engrailed* (*en*)*-Gal4* (Mark Peifer) (36), and UAS-green fluorescent protein (GFP) transgenic strains. *UAS-actin-GFP* (Mark Peifer) was used in the live imaging experiments. The following trachea-expressed *lacZ* enhancer trap and transgenic lines were crossed into a dys^2 mutant background: *Fusion-4* (*members only* [*mbo*]), *Fusion-5* (*bloated tubules* [*blot*]), *Antifusion-1* (*CrebA*), and *Terminal-3* (*ribbon*) (all from Mark Krasnow) and *shg-lacZ* (Shigeo Hayashi) (26, 31). All *dys* mutant strains were balanced over $P[w^+$; *Kr-Gal4 UAS-GFP]* (3) so that homozygous mutant embryos could be unambiguously identified.

Isolation of EMS-generated *dys* mutants. Mutations in *dys* were identified in a two-step procedure in which EMS mutations were screened over *Df(3R)Espl3* for lethality and then examined for tracheal fusion defects. Isogenic *w*; e^s males were starved overnight and then fed a 1% sucrose solution with 25 mM EMS (Sigma) for 12 h. The mutagenized (*) males were then mated en masse to *w*; *D/TM3* females. Male progeny (10,000) of the genotype *w*; e^s */TM3* were individually crossed to *Df(3R)Espl3/TM3 e* $P[w^+$; *Kr-Gal4 UAS-GFP]* females. Males were discarded, and lack of complementation to *Df(3R)Espl3* was assayed by scoring the vials for the absence of Sb^+ flies. Mutant stocks (e^s */TM3 e* $P[w^+$; *Kr-Gal4 UAS-GFP]*) were generated from 53 vials with no Sb^+ flies. Stocks were crossed inter se for complementation and representatives of each complementation group crossed to *Df(3R)Exel6204* and *Df(3R)ME61* for further genetic mapping. Members of each complementation group were assayed for tracheal fusion defects resembling the *dys* RNAi fusion defect (12).

Phenotypic analysis of larvae. Second-instar larvae homozygously mutant for *dys* were placed onto grape juice agar plates and chilled at 4°C for 30 min. The larvae were then transferred to a slide and covered in 70% glycerol, and their trachea were examined by bright-field microscopy.

DNA sequence analysis of *dys* mutants. Sequence analysis of the *dys* gene in *dys* mutant strains was carried out on genomic DNA isolated from homozygous *dys* EMS mutant embryos. The mutant embryos, balanced over $P[w^+$; *Kr-Gal4 UAS-GFP]*, were examined under a GFP stereoscope and selected manually by their absence of GFP fluorescence. The genomic DNA used as a template for PCRs encompassed the coding sequence and splice sites for all 10 *dys* exons.

Immunostaining and in situ hybridization of embryos. Whole-mount embryos were immunostained and hybridized by in situ hybridization using standard techniques (13, 22). The following primary antibodies were used for immunostaining: anti-DSRF mouse monoclonal antibody (MAb) (Active Motif), rat anti-Dys, rabbit anti-Dys, MAb 2A12, rabbit anti-diphospho-extracellular signal-regulated kinase (Sigma E7028), anti-Tgo MAb, anti-β-galactosidase MAb, rabbit anti-β-galactosidase, and rat anti-Trh. The following secondary antibodies were used: Alexafluor 546-labeled anti-mouse immunoglobulin M (IgM), Alexafluor 488-labeled anti-rat IgG, and Cy5-labeled anti-rabbit IgG. Plasmids containing *apontic* (*apt*), *btl*, *center divider* (*cdi*), *CG13196*, *CG15252*, *dys*, *esg*, *headcase* (*hdc*), *knirps* (*kni*), *knirps-related* (*knrl*), *trh*, and *ventral veinless* (*vvl*) cDNA clones (all from Origene except *dys*) were used to generate RNA probes for in situ hybridization. Embryos were examined using a Zeiss 510 confocal microscope.

Generation of *UAS-dys* transgenes. *UAS-dys* and *UAS-*Δ*b-dys* transgenes were generated for misexpression experiments. A cDNA fragment containing a copy of the *dys* coding region was cloned into the EcoRI site of pUAST (2) to create *UAS-dys*. The *UAS-*Δ*b-dys* transgene contained a copy of the *dys* coding sequence with a deletion of the entire Dys basic region (ANKSTKGASKMRR) cloned into the XbaI site of pUAST. Two *UAS-dys* lines were analyzed and showed similar tracheal defects. Seven *UAS-dys-*Δ*b* lines were analyzed; all had the same wild-type tracheal morphology upon misexpression.

Time-lapse observations of tracheal branch migration and fusion. Imaging of tracheal migration and fusion was carried out by examining wild-type and *dys* mutant *P[btl-Gal4] P[UAS-actin-GFP]* embryos, in which *actin-GFP* was expressed in the trachea (24). The *dys* mutant chromosome was balanced over *TM3 P[Kr-Gal4] P[UAS-GFP]*. Homozygous *dys* mutants were identified because of cortical actin-GFP in the trachea, due to *UAS-actin-GFP* expression, whereas nonmutant embryos with one or two copies of *TM3 P[Kr-Gal4] P[UAS-GFP]* showed cytoplasmic GFP in the trachea, due to the presence of cytoplasmic GFP driven by *btl-Gal4* acting on *P[UAS-GFP]*. Embryos were collected at room temperature and dechorionated. They were then mounted on a glass coverslip and immersed in halocarbon oil 700 (Sigma) on slides containing an oxygen-permeable membrane. GFP fluorescent images were captured on a Zeiss LSM-510 confocal microscope with a 60× oil immersion lens for 2 h (wild-type embryos) and 4 h (*dys* mutant embryos). Typically, projections consisted of ten 2-μm slices captured along the *z* axis every 2 min for wild-type embryos and every 4 min for *dys* mutant embryos. Movies were assembled from projections by using Image J software.

RESULTS

Isolation of *dys* mutant alleles. The strategy for isolating *dys* mutants was based on RNAi results. Previously, it was shown that injection of *dys* double-stranded RNA into *Drosophila* embryos resulted in (i) a loss of detectable Dys protein, (ii) embryonic and larval tracheal fusion defects, and (iii) a high degree of larval lethality (12). These results provided the basis for an EMS screen for *dys* mutants (Fig. 1), based on *dys* being a vital locus with easily detectable tracheal defects. In our screen, mutagenized males were crossed to a deletion strain, *Df(3R)Espl3*, that removes *dys*, and stocks that failed to complement the deficiency strain were screened for tracheal defects. Representative mutant larvae from each complementation group were analyzed for tracheal defects by examination with phase-contrast microscopy. Mutant larvae from group 3 (Table 1), which contains nine different mutants, had tracheal fusion defects (Fig. 2A to F) identical to those observed in the *dys* RNAi embryos (12). Identical, severe tracheal fusion phenotypes were observed in homozygous mutants of all nine *dys*

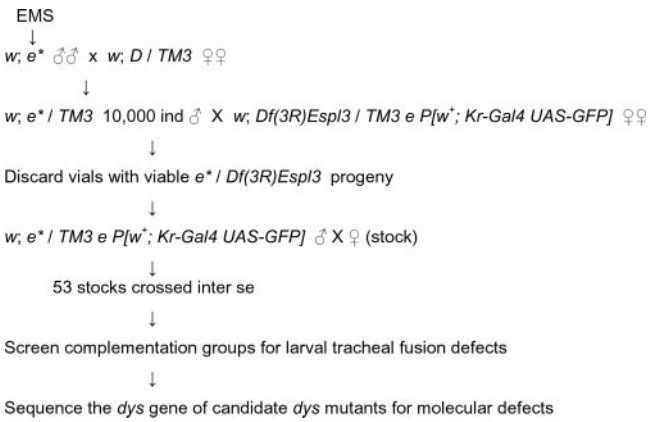

FIG. 1. Isolation of EMS-mutagenized *dys* alleles.

alleles, when examined as either second-instar larvae or stage 17 embryos. Embryos heterozygous for combinations of two different *dys* alleles and *dys*/*Df(3R)Espl3* mutants all showed similar severe phenotypes identical to those of homozygous *dys* mutants. Thus, all mutants appear to have a severe, genetically null *dys* phenotype. *dys* mutant strains are lethal, with animals dying as second- or third-instar larvae.

DNA sequence analysis of *dys* exons and intron/exon boundaries derived from homozygous mutant embryo genomic DNA was used to confirm that complementation group 3 mutants corresponded to the *dys* gene. The results are summarized in Fig. 3. Three alleles have premature stop codons: dys^2 and dys^3 have termination codons in the HLH region, and dys^7 has a termination codon in the PAS-2 domain. Three alleles, dys^4, dys^5, and dys^6, have mutations that likely affect splicing and would result in proteins truncated within or at the end of the PAS-2 domain. The remaining three alleles show no obvious mutation in the coding region or splice sites. All six *dys* alleles with recognizable mutations are predicted to produce truncated proteins that lack the C-terminal region, which was used as an antigen to generate Dys antibody (Fig. 3). Consistent with the sequencing data, no Dys immunoreactivity was detected in homozygous mutant embryos from any of these strains (data not shown). Wild-type levels of *dys* RNA were present in the two *dys* mutants assayed, dys^2 and dys^3, suggesting that *dys* expression is not maintained in tracheal cells by positive autoregulation (data not shown).

***dys* mutants show tracheal adhesion and fusion defects.** *dys* mutants were initially examined for larval defects in tracheal fusion (Fig. 2A to F). The GBs, DBs, and LT branches in *dys* mutant embryos showed a complete absence of fusion in all branches examined. The dorsal trunk (DT) (Fig. 2B) was fused and relatively normal in appearance, although some DT fusion sites were constricted (Fig. 2D). These results were identical to those observed with the *dys* RNAi experiments (12). Penetrance and expressivity were 100% for dys^2/dys^3 mutant larvae, as well as for other *dys* alleles and allelic combinations analyzed. In each case, the mutant tracheal branches had migrated near the point of fusion but failed to fuse. These results were confirmed by staining stage 16 embryos with MAb 2A12, which stains the tracheal lumen (Fig. 2G and H). Mutant embryos showed an absence of fusion by stage 16.

More-detailed analyses of *dys* mutant embryos were carried out by employing time-lapse microscopy of tracheal migration and fusion (Fig. 4 and data not shown). Wild-type and *dys* mutant embryos containing *btl-Gal4 UAS-actin-GFP* were visualized for GFP fluorescence by using confocal microscopy and compared over 4 h of development with respect to migration, filopodial dynamics, and fusion. The *btl-Gal4* transgene expresses *Gal4* in most tracheal cells, and *UAS-actin-GFP* allows visualization of actin-rich structures, including tracheal filopodia (24). We focused on the DB, which migrates over large distances along the internal surface of the dorsal epidermis to meet and fuse at the dorsal midline with its partner from the adjacent hemisegment. In both wild-type and *dys* mutant embryos, the migratory processes, including filopodial extension, were similar. However, in wild-type embryos, the filopodia from the fusion cells touched and adhered, and the fusion cells joined together (Fig. 4A to E). The fusion event was accompanied by intense actin accumulation at the fusion junction. In mutant embryos (Fig. 4F to N), the two fusion cells migrated close to each other, and filopodia made contact. However, the cells failed to adhere and remained separated. In summary, the time-lapse movies indicated that long-range migration in *dys* mutant embryos is sufficiently normal that fusion cells contact each other via their filopodia. However, the branches fail to stably adhere and fuse.

Misexpression of *dys* results in ectopic fusion and inhibition of tracheal migration and lumen formation. Additional insight into the function of *dys* was obtained by misexpressing the gene in trachea by using *UAS-dys* transgenic fly strains crossed to *btl-Gal4*. This results in *dys* being expressed at high levels in most tracheal cells (Fig. 5A). Staining of w^- control embryos with MAb 2A12 revealed the characteristic and extensive secondary and tertiary branches and branch fusion (Fig. 5B). However, MAb 2A12 staining and examination of GFP in *btl-Gal4 UAS-dys UAS-GFP* embryos indicated a striking re-

TABLE 1. Mutants isolated in the EMS mutagenesis

Complementation group[a]	Mutant(s)
Df(3R)Exel6204	
1	1, 13
2 (*gro*)	2, 3, 16, 17, 18, 26, 27, 28, 31, 33, 43, 45, 59
3 (*dys*)	4, 6, 14, 35, 42, 51, 53, 54, 57
4	5, 15, 20, 34, 39, 40, 52, 55
5	7, 12, 60
6	8, 11, 19, 23, 32, 46, 56
7	9, 10, 49
8	38, 44, 47, 48
9	41
10	58
Df(3R)Espl3	
11	21
12	24
13	30
14	37
15	50

[a] Fifty-three mutants failed to complement *Df(3R)Espl3* [96F1; 97B1]. These mutants were crossed inter se and placed into 15 complementation groups numbered 1 to 15. Ten of those complementation groups also failed to complement *Df(3R)Exel6204* [96F9; 97A6], and five lie outside that chromosomal interval. The group 3 mutants were named *dys to dys* in ascending order. Complementation group 2 contains alleles of *groucho* (*gro*).

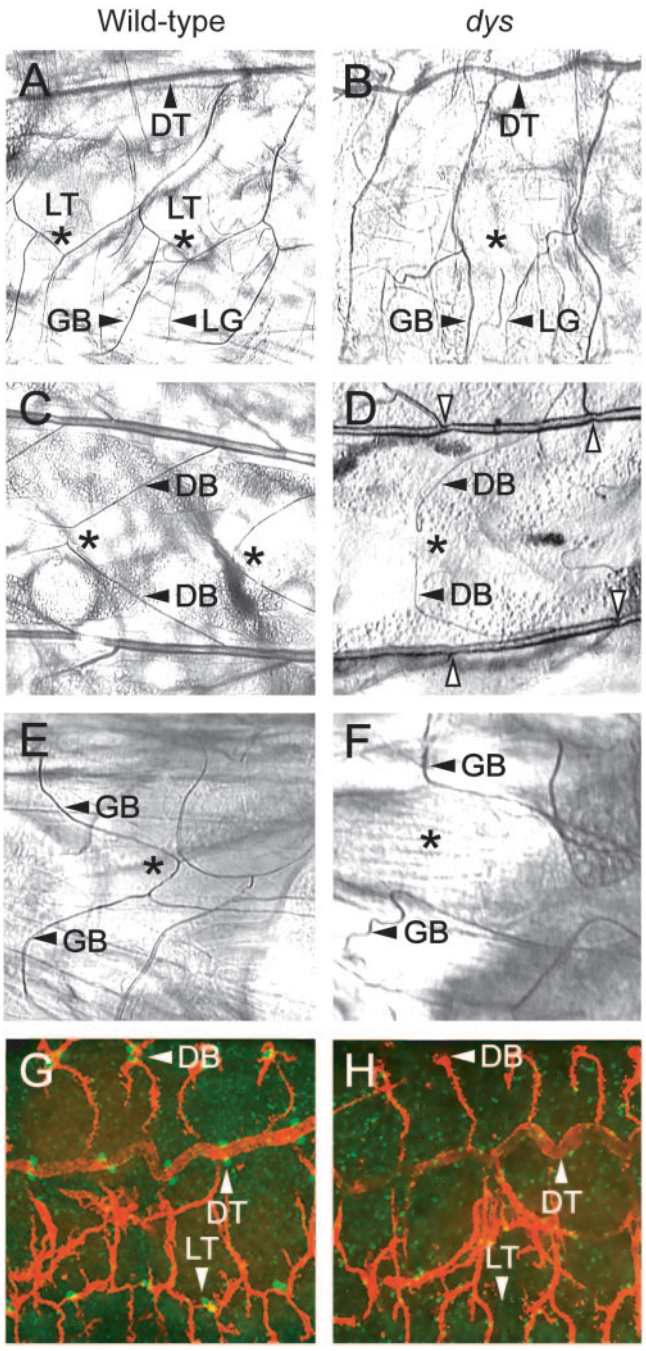

FIG. 2. *dys* mutant embryos show tracheal fusion defects. Anterior is to the left in all panels. (A to F) Trachea from wild-type and dys^2/dys^3 mutant second-instar larvae were examined by phase microscopy. (A and B) Sagittal view. (A) The LT is fused (*) in a wild-type larva. The DT, GB, and lateral branch G (LG) are shown. (B) A *dys* mutant larva shows an absence of LT fusion (*). The GB and LG branch still persist and project ventrally. The DT is fused. (C and D) Dorsal view. (C) Wild-type larva showing fusion (*) of the DBs. (D) *dys* mutant larva showing a lack of DB fusion (*), although branches (arrowheads) are close together. Constrictions are seen in *dys* mutant DTs at fusion sites (open arrowheads). (E and F) Ventral view. (E) Wild-type larva showing fusion (*) of GBs. (F) *dys* mutant larva showing a lack of GB fusion (*). (G and H) Sagittal view. Confocal microscopic analysis of whole-mount embryos. (G) Stage 16 wild-type embryo stained with MAb 2A12 (red) and anti-Dys (green), showing fusion (arrowheads) of DBs, DTs, and LTs. Mab2A12 stains the tracheal lumen, and anti-Dys stains the tracheal fusion cells. (H) Stage 16 *dys* mutant embryo stained with MAb 2A12 (red) and anti-Dys (green), showing an absence of fusion of DB and LT branches. The DT is fused. Note the absence of anti-Dys reactivity.

duction in DB, DT, GB, and visceral branch branching (Fig. 5C and D). While both DT and LT branches were sometimes fused, the connections were abnormal and were characterized by reduced GFP-positive cytoplasmic material and an absence of MAb 2A12 luminal staining. The *dys* misexpression embryos also resulted in the formation of ectopic tracheal fusion events, connecting tracheal branches that normally never join (Fig. 5E and F). These ectopic fusion events rarely showed the presence of MAb 2A12 luminal staining at the fusion sites. The *dys* misexpression experiments provided evidence that *dys* can promote tracheal fusion events, consistent with the *dys* mutant studies. However, the misexpression experiments also provided evidence that tracheal migration can be inhibited by *dys*.

The biochemical mechanism of the *dys* misexpression phenotypes (and thus likely to be relevant to the *dys* mutant phenotypes) was assessed using a mutant version of *dys* that lacks the putative DNA binding basic region (Δ*b-dys*) in the *dys* misexpression assay. Embryos that were *btl-Gal4 UAS-*Δ*b-dys* showed trachea that were wild type in appearance (Fig. 5G and H). The Δ*b-dys* gene was misexpressed at high levels as revealed by anti-Dys immunostaining of misexpression embryos (Fig. 5H), and it was able to dimerize with Tgo and translocate to the nucleus as revealed by staining *en-Gal4 UAS-*Δ*b-dys* embryos with anti-Tgo (data not shown). Thus, the inability of Δ*b-dys* to generate misexpression phenotypes is likely due to its inability to bind DNA. While the relationship between the *dys* misexpression and mutant phenotypes is uncertain, these results indicated that the ability of *dys* to inhibit cell migration and promote tracheal fusion requires the ability to bind DNA.

Regulation of fusion cell gene expression by Dys. Since Dys is a transcription factor expressed in tracheal fusion cells, important insight into its biological function can be revealed by identifying transcriptional target genes. We examined 19 trachea-expressed genes in both wild-type and *dys* mutant embryos for potential regulation by *dys*. The genes fall into three categories: (i) those prominently expressed in fusion cells, (ii) those expressed in terminal cells but not fusion cells, and (iii) those expressed in tracheal cells but downregulated in fusion cells.

(i) Fusion cell-expressed genes. Previous work identified a number of fusion cell-expressed genes that are regulated by *esg* (27), including *blot*, *dys*, *hdc*, *mbo*, and *shg*. Another trachea-expressed gene, *cdi*, is not regulated by *esg*. Expression of these genes, and also *esg*, *CG13196* (a ZP family gene expressed in fusion cells) (11), and *CG15252* (which encodes a protein of unknown function) (32), was examined in *dys* mutant embryos. Four genes, i.e., *shg*, *CG13196*, *CG15252*, and *mbo* (Fig. 6A to E) were found to be regulated by *dys*, whereas the other five, i.e., *blot*, *cdi*, *dys*, *esg*, and *hdc*, were not regulated by *dys* (data not shown). The expression of *shg* is upregulated by *dys* from a basal level, whereas *dys* is required for the initiation of *CG13196*, *CG15252*, and *mbo* expression. *shg* expression is enhanced in both DB and DT fusion cells, but *dys*

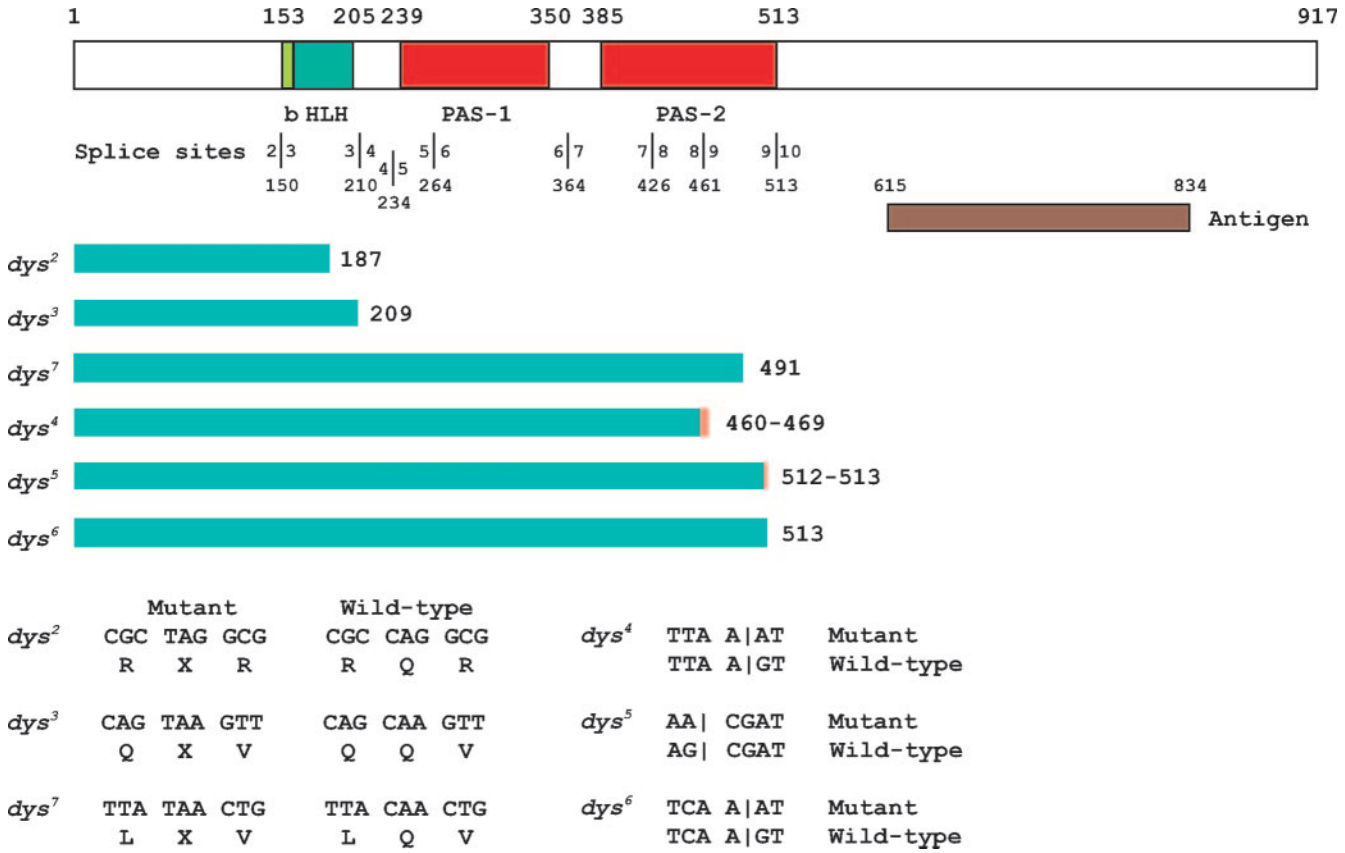

FIG. 3. Molecular defects of *dys* mutants. At the top is a schematic of the Dys protein. The basic-region DNA binding domain (b), HLH dimerization domain, and PAS-1 and PAS-2 domains are labeled below the schematic. Above the schematic are the amino acid positions of domain boundaries. The locations of splice sites are shown below the domain names, and each exon-intron boundary is indicated by a vertical line with the corresponding exon indicated on each side, along with the amino acid residue corresponding to the splice site below. The anti-Dys antibody was raised against animals injected with a bacterial fusion protein antigen containing Dys protein residues 615 to 834. The conceptual protein fragment predicted for each *dys* mutant gene is indicated by a green bar, followed by the size in amino acids. The minimum extent of the predicted protein is shown in green, and the orange bar indicates translated intronic sequences. dys^2, dys^3, and dys^7 have premature termination codons that should result in a truncated protein. dys^4, dys^5, and dys^6 have splice site mutations. dys^4 and dys^5 are followed by two numbers; the first indicates the end of the exonic sequence and the second the location of the in-frame termination codon in the adjacent intron. The sequence alteration for each mutant is shown at the bottom. Vertical lines for dys^4, dys^5, and dys^6 indicate locations of splice sites.

(as well as *esg* [31]) controls expression in only DBs and not DTs. *shg* and *CG13196* are membrane proteins that may control fusion cell recognition and adhesion events, whereas *mbo* attenuates protein nuclear export. Levels of *shg* and *mbo* were assayed by examining *shg-lacZ* and *mbo/Fusion-4-lacZ* lines, indicating that the control by *dys* is likely to be at the transcriptional level.

The *shg* gene encodes a cadherin cell adhesion protein implicated in tracheal morphogenesis and branch fusion (31, 33). *CG13196* encodes a ZP protein of unknown function. An attempt to abolish *CG13196* function by using RNAi showed only weak effects on tracheal fusion (data not shown). In contrast, misexpression of *CG13196* in *btl-Gal4 UAS-CG13196* embryos revealed sites of ectopic fusion (Fig. 6F), suggesting that *CG13196* encodes an adhesion protein. This suggests that Dys controls expression of a group of two or more proteins involved in tracheal recognition/adhesion events.

(ii) Terminal cell-expressed genes. While screening for genes expressed in tracheal cells, Samakovlis et al. (26) identified a class of trachea-expressed genes that were expressed in terminal cells, which in the case of DBs are adjacent to fusion cells. Analysis of two terminal-class genes, including *DSRF*, in *esg* mutants indicated that *esg* represses expression of both genes in fusion cells. We investigated whether terminal genes, including *DSRF* and *ribbon*, were negatively regulated by *dys* in fusion cells. In both cases, expression was unaffected in fusion cells (data not shown). While this analysis is limited to these two genes, it indicates that the negative regulation of *DSRF* in fusion cells by *esg* is not mediated by *dys*, and transcriptional repression in fusion cells may not be a common role of *dys*.

(iii) Fusion cell-downregulated genes. We examined expression of a number of genes that are broadly expressed during tracheal development and found that downregulation in fusion cells is common. These genes included six that encode transcription factors: *apt*, *crebA* (*Antifusion-1*), *kni*, *knrl*, *trh*, and *vvl* (Fig. 6G to J). In addition, expression of the *btl* receptor, which is a direct transcriptional target of Trh, was downregulated (Fig. 6K). Consistent with a reduction in *btl*, mitogen-activated protein kinase (MAPK) activation, as assayed by immunostaining for phosphorylation with anti-diphospho-MAPK, was also reduced (data not shown), as noted previously (9). When

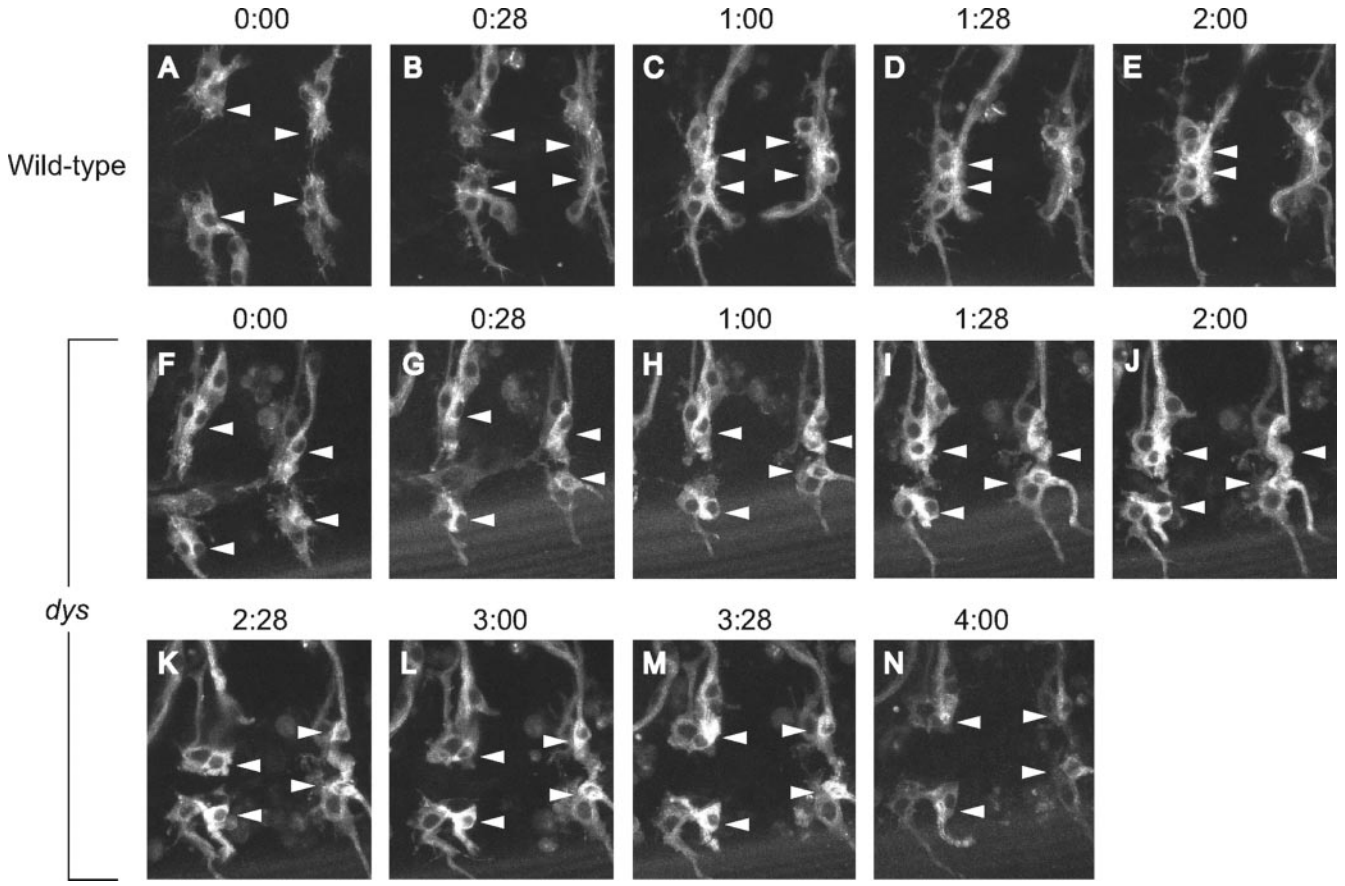

FIG. 4. Live imaging of wild-type and *dys* mutant tracheae. DB migration and fusion were examined by live confocal imaging of tracheal GFP fluorescence. Shown are individual images from a wild-type *btl-Gal4 UAS-actin-GFP* embryo (A to E) imaged over 2 h and a dys^2/dys^3 *btl-Gal4 UAS-actin-GFP* mutant embryo (F to N) imaged over 4 h. Filopodia from tip/fusion cells (arrowheads) can be observed in both migrating wild-type (A and B) and *dys* mutant (F to N) trachea. Note the accumulation of actin-GFP at sites of fusion in wild-type embryos (C to E). In the *dys* mutant embryo, the fusion cells come into close range (F to N) but fail to form stable contacts.

tested in *dys* mutants, transcript levels of all eight genes plus the diphospho-MAPK gene remain reduced, indicating that the downregulation is not *dys* dependent (data not shown).

It was noted previously that in wild-type embryos Trh protein levels were reduced in fusion cells (Fig. 6L1 and M1), and injection of *dys* RNAi restored Trh protein levels to the levels found in the adjacent tracheal cells (12). Using *dys* mutant and misexpression embryos, Trh protein levels were examined in fusion cells. In *dys* mutant embryos, Trh proteins levels were comparable to the levels observed in adjacent cells in DTs (Fig. 6L2) and DBs (Fig. 6M2). Misexpression of *dys* in *btl-Gal4 UAS-dys* embryos also showed a reduction in Trh protein levels (Fig. 6N1 to 3). In contrast, *trh* RNA levels were not affected in either *dys* mutant or misexpression embryos (data not shown). Misexpression of Δ*b-dys* did not result in a reduction of Trh protein levels (Fig. 6N4), indicating that Trh protein reduction requires Dys DNA binding and transcriptional regulation. Since Trh protein levels, but not RNA levels, are negatively regulated by Dys transcriptional activity, most likely Dys activates transcription of an unknown gene, whose function is to regulate Trh protein levels.

Misexpression of *dys* results in ectopic expression of Dys target genes. *CG13196* is expressed in all tracheal fusion cells (Fig. 7A), and *CG15252* is expressed only in DT fusion cells (Fig. 7D). Expression of both genes was assayed in *btl-Gal4 UAS-dys* embryos. *CG13196* was robustly misexpressed throughout the trachea, including all primary branches (Fig. 7B). *CG15252* was misexpressed, but the misexpression was restricted mainly to DTs and some cells in the adjacent transverse connective (Fig. 7E). Clearly absent was *CG15252* expression in DBs, LTs, and GBs. The *esg* gene, which is expressed in fusion cells but is not a Dys target gene, was not ectopically expressed in *btl-Gal4 UAS-dys* embryos (not shown). Thus, ectopic tracheal gene expression by Dys seems specific for Dys target genes and not for all fusion cell-expressed genes. *CG13196* and *CG15252* expression required Dys DNA binding, since misexpression of *dys*-Δ*b* failed to activate their transcription (Fig. 7C and F). Neither gene is expressed in nontracheal sites of *dys* expression, such as leading-edge and anal pad cells, nor does *btl-Gal4 UAS-dys* central nervous system midline cell expression result in ectopic expression of *CG13196* or *CG15252* in the central nervous system midline cells. Thus, while Dys:Tgo is able to efficiently activate transcription of fusion cell target genes throughout the trachea, it is unable to activate them indiscriminately in all cell types.

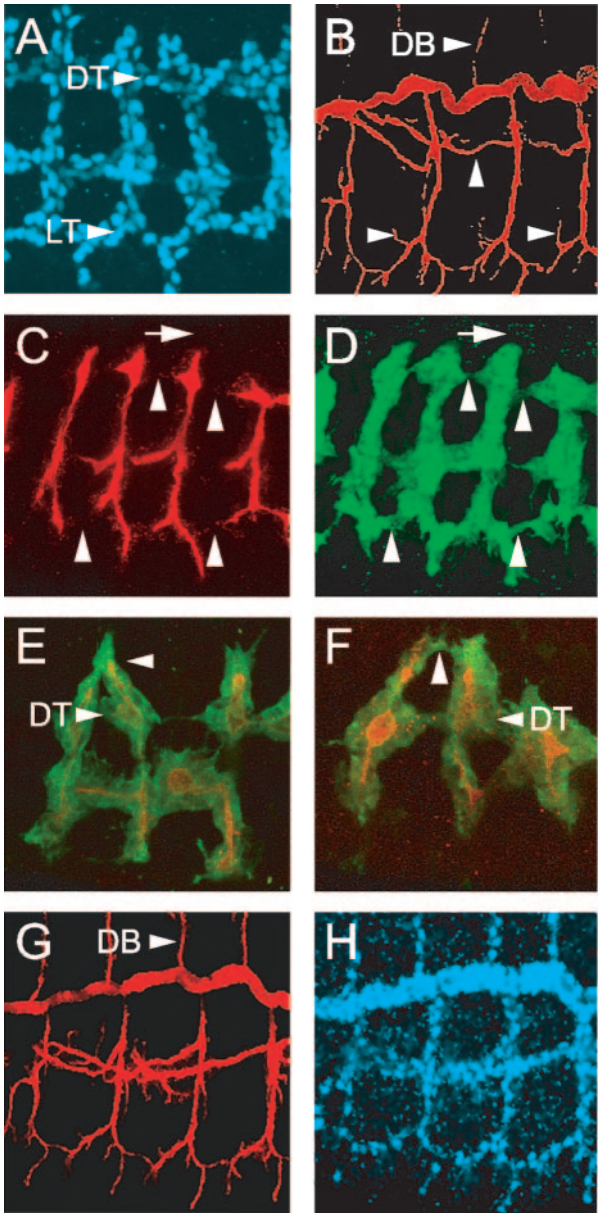

FIG. 5. Misexpression of *dys* results in tracheal fusion, migration, and lumen formation defects. All embryos are stage 16, and sagittal views are shown. Embryos were stained with combinations of MAb 2A12 (red), anti-Dys (blue), and anti-GFP (green). (A) *btl-Gal4 UAS-dys* embryo showing the strong misexpression of Dys protein throughout the trachea. The DT and LT are indicated. (B) w^- control embryo. Note the extensive branching (arrowheads) illustrated by MAb 2A12 staining, including DBs. (C and D) *btl-Gal4 UAS-dys UAS-GFP* embryo. (C) MAb 2A12 staining reveals that the trachea shows a severe reduction in secondary and tertiary branching, as well as breaks in lumen formation at normal sites of fusion (arrowheads). Both DBs and GBs are severely stunted (arrows in C and D show lack of DB extension; compare to panels B and G). (D) Staining for cytoplasmic GFP shows that both the DT and LT are often joined at fusion sites, but (C) show an absence of MAb 2A12 luminal staining. (E and F) Two *btl-Gal4 UAS-dys UAS-actin-GFP* embryos. Arrowheads point to sites of ectopic fusion. While the cytoplasmic GFP staining is continuous, MAb 2A12 luminal staining is absent at fusion sites. The DT is indicated. (G and H) *btl-Gal4 UAS-dys-Δb* embryo. The trachea has a wild-type pattern of branching.

DISCUSSION

The isolation of *dys* mutants allowed detailed phenotypic analysis using time-lapse confocal microscopy of live embryos. Migration and the presence of filopodia during DB branching appeared normal in *dys* mutant embryos. The two DB fusion cells moved close together, and their filopodia were observed to touch. However, unlike wild-type cells, the *dys* mutant fusion cells failed to stably adhere. Thus, no fusion occurred, and ultimately the branches retracted from one another. Additional insight into the role of *dys* emerged from experiments in which *dys* was misexpressed throughout the trachea. Ectopic fusion events were observed, which is consistent with the *dys* mutant phenotype and indicates that *dys* promotes fusion cell recognition/adhesion. In addition, *dys* misexpression results in a strong reduction in both tracheal branching and formation of MAb 2A12 luminal material at fusion sites. The reduction in branching suggests that another possible function of *dys* is to inhibit migration in preparation for fusion. The reduction in MAb 2A12 luminal material at sites of normal and ectopic fusion suggests that the fusion process is incomplete. This can be explained for the ectopic fusion results by proposing that Dys activates genes that can mediate fusion but not lumen formation. Since the ectopic cells are not fusion cells, the additional lumen-forming functions would not be present. In contrast, since lumen formation was also defective at normal fusion sites, it is possible that Dys overexpression inhibits lumen formation. In summary, the genetic and misexpression experiments suggest that *dys* is activated late in the branching process to inhibit migration and promote branch recognition and adhesion. It may also play additional roles after branches join.

Since *dys* encodes a transcription factor, it is expected that it functions by regulating gene expression. Previous work had identified several genes prominently expressed in fusion cells, as well as additional trachea-expressed genes whose fusion cell expression was low or absent (26, 31). In this paper, we further showed that a number of prominent trachea-expressed genes are also downregulated in fusion cells, indicating that this is a common occurrence. Expression of 19 genes was assayed in *dys* mutant embryos to identify Dys target genes. RNA levels of four genes (*CG13196*, *CG15252*, *mbo*, and *shg*) were reduced. In contrast, Trh protein levels, which normally decline in fusion cells, increased in *dys* mutants. These results were confirmed by *dys* misexpression experiments, in which *CG13196* and *CG15252* were increased and Trh protein levels declined. Despite *dys* expression in all tracheal fusion cells, there exist branch-specific differences in Dys-regulated gene expression. *CG13196* is expressed in all fusion cells, and *dys* is required for its expression. In contrast, *shg* is upregulated in DB and DT fusion cells, but only DB upregulation requires Dys, an effect also seen for Esg (31). *CG15252* is expressed only in DT fusion cells, and this restriction may be due to the positive or negative action of branch-specific transcription factors, such as Spalt major (DT specific, positively acting) (7, 15) or Kni and Knrl (non-DT branches, negatively acting) (5, 18).

All of the *dys* misexpression defects (and thus probably the mutant defects) require Dys DNA binding, since deletion of the *dys* basic region, and presumably its ability to bind DNA, abolishes the tracheal defects. Although *trh* RNA levels de-

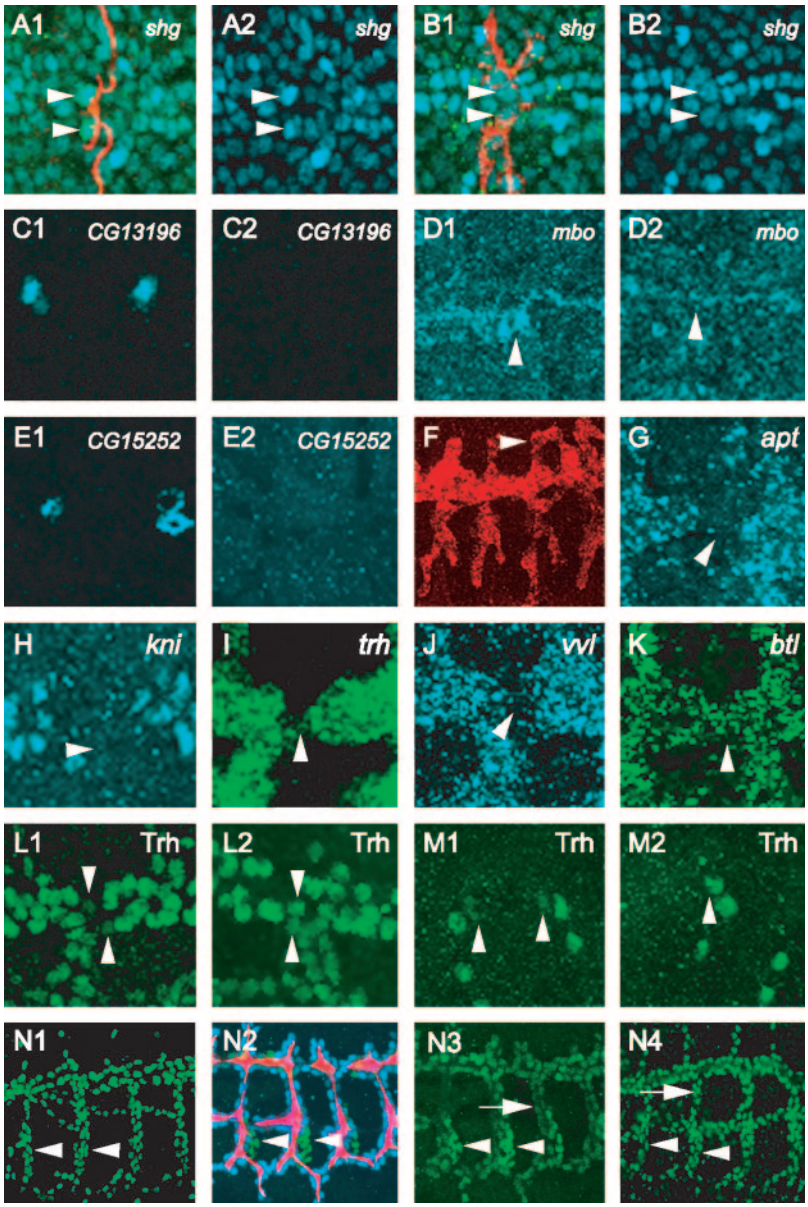

FIG. 6. Regulation of gene expression in tracheal fusion cells. Each panel consists of a projection of three consecutive 1-μm confocal slices. (A to D) *shg* upregulation in DBs is dependent on *dys* function. Stage 16 *shg-lacZ* embryos were stained with anti-β-galactosidase (A1 and B2; blue), MAb 2A12 (A1 and B1; red), and anti-Dys (not shown). The use of anti-Dys staining allows for selection of homozygous mutant embryos, since they do not possess antibody-reactive protein. Fusion cells (arrowheads) express a higher level of β-galactosidase than surrounding tracheal cells in wild-type DB (A1 and A2). This upregulation was not observed in *dys* mutant DB fusion cells (B1 and B2, arrowheads). (C1 to M2) Embryos were hybridized to gene-specific probes and a *dys* RNA probe and immunostained with anti-Dys. *dys* RNA hybridization revealed fusion cells, and anti-Dys allowed identification of *dys* mutant embryos. (C1 and C2) *CG13196* fusion cell expression is dependent on *dys*. Stage 15 wild-type DT fusion cells express *CG13196* (C1), but *dys* mutants (C2) do not. (D1 and D2) *mbo* expression is regulated by *dys*. *Fusion-4* embryos, which contain an *mbo-lacZ* enhancer trap gene, were immunostained with anti-β-galactosidase. Stage 15 wild-type DT (D1) fusion cells (arrowheads) show high levels of *lacZ* expression, whereas β-galactosidase expression is absent in *dys* mutant DT (D2). (E1 and E2) *CG15252* fusion cell expression is dependent on *dys*. Stage 15 wild-type DT fusion cells (E1) express *CG15252*, but *dys* mutants (E2) do not. (F) Misexpression of *CG13196* in *btl-Gal4 UAS-CG13196* embryos results in ectopic tracheal branch fusion (arrowhead). (G to K) Stage 15 embryos were hybridized to *apt* (G), *kni* (H), *trh* (I), *vvl* (J), and *btl* (K) probes as well as to a *dys* probe to mark fusion cells (not shown). RNA levels of all five genes are downregulated in fusion cells but are not regulated by *dys* (not shown). (L1 to M2) *dys* downregulates Trh protein levels. Trh protein levels are reduced in wild-type (L1) DT fusion cells (arrowheads) and (M1) DB fusion cells (arrowheads). In *dys* mutant embryos, Trh proteins levels increased to levels comparable to those in other tracheal cells in both DTs (L2) and DBs (M2). (N1 to N4) Embryos stained with ant-Trh (green). (N1) w^- control embryo. Trh is localized to nuclei at uniform levels throughout the trachea. Cells of the spiracular branch (arrowheads) show the same levels of Trh as other tracheal cells. (N2 and N3) *btl-Gal4 UAS-dys* embryo. (N2) Embryo stained with MAb 2A12 (red), anti-Dys (blue), and anti-Trh (green). *btl-Gal4 UAS-dys* is expressed at high levels in all tracheal cells except the spiracular branch cells (green; arrowheads). (N3) Trh levels are reduced in *dys*-positive cells (arrow) compared to spiracular branch cells (arrowheads). (N4) *btl-Gal4 UAS-dys-Δb* embryo. Trh levels are uniform throughout the trachea, as indicated by comparable Trh levels in *dys*-positive cells (arrow) compared to spiracular branch cells (arrowheads).

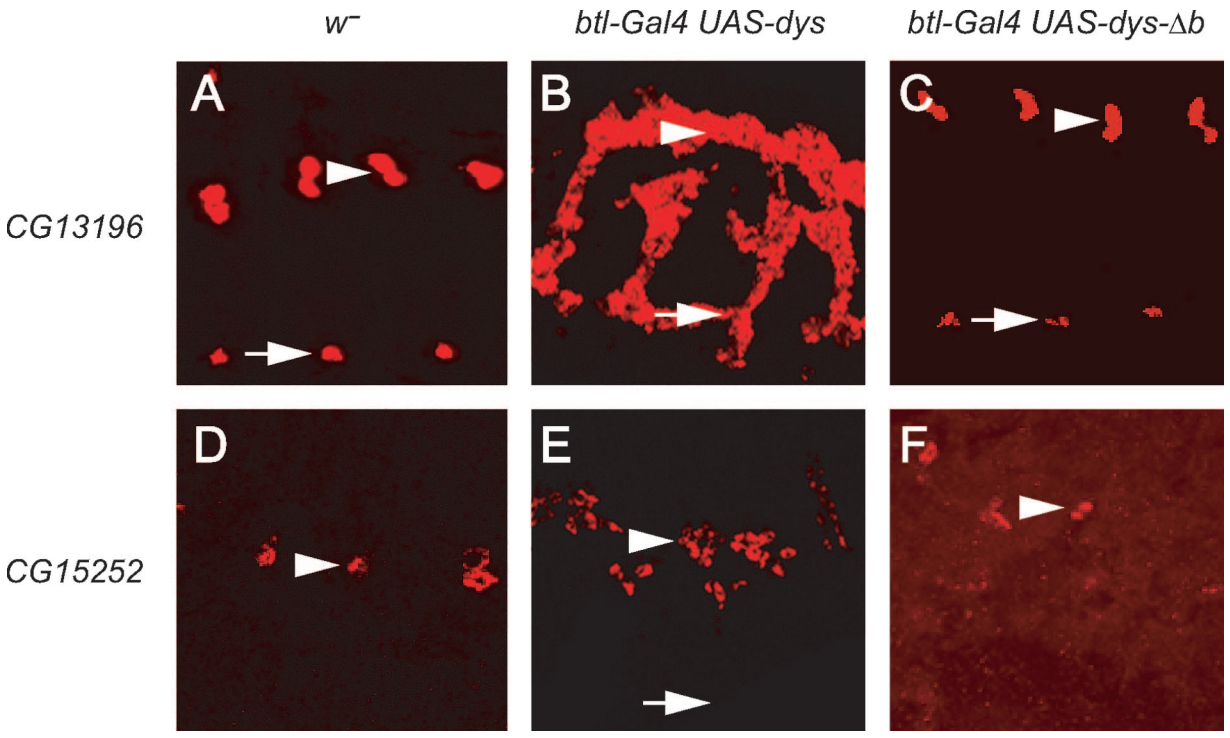

FIG. 7. Misexpression of *dys* in trachea results in ectopic expression of *dys* target genes. All panels show sagittal views of stage 16 embryos; anterior is to the left. Positions of DTs (arrowheads) and LTs (arrows) are indicated. (A to C) w^- (A), *btl-Gal4 UAS-dys* (B), and *btl-Gal4 UAS-dys-Δb* (C) embryos were hybridized to a *CG13196* probe (red). Embryos were also stained with anti-Dys to monitor misexpression (not shown). (A) In w^- control embryos, *CG13196* is expressed in fusion cells of DTs and LTs. (B) *CG13196* expression is found throughout the trachea when *dys* is ectopically expressed. (C) Only wild-type expression of *CG13196* in DTs and LTs is observed when *dys-Δb* is misexpressed. (D to F) w^- (D), *btl-Gal4 UAS-dys* (E), and *btl-Gal4 UAS-dys-Δb* (F) embryos were hybridized to a *CG15252* probe (red). (D) *CG15252* is expressed only in DT fusion cells in w^- control embryos. (E) *CG15252* expression is ectopically expressed when *dys* is misexpressed in all tracheal cells, but it is restricted to DT and some nearby tracheal cells. It is completely absent from LTs and GBs. (F) *CG15252* expression is restricted to DT fusion cells and is not ectopically expressed in *btl-Gal4 UAS-dys-Δb* embryos.

cline in fusion cells along with protein levels, the RNA reduction is not *dys* dependent. Thus, *dys* likely regulates transcription of a gene that regulates Trh protein levels. Similarly, the requirement of Dys DNA binding to regulate Trh protein levels does not support a model (12) in which Trh levels are reduced as a consequence of Dys competing for their common dimerization partner, Tgo, since this is unlikely to require DNA binding.

The recognition/adhesive properties promoted by *dys* may be mediated by two Dys target genes, *shg* and *CG13196*. Shg is a well-studied adhesion protein, and *CG13196* encodes a ZP transmembrane protein, although its function and subcellular localization are unknown. Misexpression of *CG13196* results in ectopic fusion events consistent with it playing a role in cell adhesion. Thus, one key role of *dys* may be to promote tracheal fusion by controlling expression of two or more cell adhesion protein genes. They could work together in the same cellular process or in different aspects of tracheal fusion, lumen formation, or function. The identification of *mbo* as a transcriptional target of Dys is intriguing, since *mbo* mutants have a tracheal fusion defect (35) and it attenuates protein nuclear export (25). Although the fusion cell protein cargo regulated by *mbo* is unknown, it presumably includes proteins that are localized to nuclei in fusion cells.

The two major transcription factors studied to date that control fusion cell transcription and development are *esg* and *dys*. *esg* precedes *dys* during fusion cell development and controls expression of *dys* in DBs and GBs but not DTs (12) (the case for LTs is unknown, since fusion cells die in *esg* mutants [27]). *dys* itself does not affect *esg* expression (12). The tracheal fusion phenotypes of both genes are similar. The DT is the one branch that still fuses in both *esg* and *dys* mutants, although both show constrictions at the sites of DT fusion (27, 31). Previous work on *esg* revealed that, genetically, it is required for both activation of fusion cell gene expression and repression of terminal cell gene expression in fusion cells (27, 31). In this study, we found that *dys* constitutes a transcriptional pathway that carries out a subset of *esg* functions, focused on upregulating expression of genes involved in cell adhesion and protein localization, although future work may uncover additional target genes. Since a large number of genes are either activated or downregulated in tracheal fusion cells (L. Jiang, unpublished data), it will be important to continue genetic and molecular studies to determine which genes are targets of Esg and Dys and whether their control is direct or indirect.

One model of *Drosophila dys* function is that *dys* acts as a developmental timer near the end of tracheal branching to inhibit migration and promote cell adhesion and fusion. The adhesion component works, in part, through activation of *shg* and (possibly) *CG13196*. The inhibition of migration has only

been postulated from misexpression experiments and needs to be confirmed by alternative approaches. It is also important to note that the switch from migration to fusion can also include changes in gene expression that are independent of *dys*. For example, it is shown here that RNA levels of *btl*, a gene required for tracheal migration, are downregulated in fusion cells in a *dys*-independent mode. *dys* is expressed in a variety of *Drosophila* embryonic cell types, including leading edge, brain, gut, and anal pad (12), and the mammalian ortholog is prominently expressed in the brain (17, 21). However, the function of *dys* in these cell types is unknown, although a potential connection between tracheal fusion cells and both migrating neuronal axon growth cones and leading-edge cells is worth investigating. The role of *dys* in controlling fusion cell behavior suggests that it is worthwhile to look in tissues that undergo branching morphogenesis, such as the vertebrate lung and vascular system, for regulatory proteins expressed in tip/fusion cells that control the migration, recognition, and fusion properties of their branches.

ACKNOWLEDGMENTS

We thank Julie Gates, Shigeo Hayashi, Tien Hsu, Mark Krasnow, Mark Peifer, Tony Perdue, Benny Shilo, Christos Samakovlis, and the Bloomington Fly Stock Center for stocks and reagents and Joseph Kearney for helpful comments on the manuscript. We remember the contributions to tracheal development by the late Peter Kolodziej, who also generously contributed advice and reagents to this project.

This project was funded by a grant from the National Science Foundation (Developmental Mechanisms) to S.T.C.

REFERENCES

1. **Arquier, N., P. Vigne, E. Duplan, T. Hsu, P. P. Therond, C. Frelin, and G. D'Angelo.** 2006. Analysis of the hypoxia-sensing pathway in Drosophila melanogaster. Biochem. J. **393:**471–480.
2. **Brand, A. H., and N. Perrimon.** 1993. Targeted gene expression as a means of altering cell fates and generating dominant phenotypes. Development **118:**401–415.
3. **Casso, D., F. Ramirez-Weber, and T. B. Kornberg.** 2000. GFP-tagged balancer chromosomes for Drosophila melanogaster. Mech. Dev. **91:**451–454.
4. **Centanin, L., P. J. Ratcliffe, and P. Wappner.** 2005. Reversion of lethality and growth defects in Fatiga oxygen-sensor mutant flies by loss of hypoxia-inducible factor-alpha/Sima. EMBO Rep. **6:**1070–1075.
5. **Chen, C. K., R. P. Kuhnlein, K. G. Eulenberg, S. Vincent, M. Affolter, and R. Schuh.** 1998. The transcription factors KNIRPS and KNIRPS RELATED control cell migration and branch morphogenesis during Drosophila tracheal development. Development **125:**4959–4968.
6. **Englund, C., P. Steneberg, L. Falileeva, N. Xylourgidis, and C. Samakovlis.** 2002. Attractive and repulsive functions of Slit are mediated by different receptors in the Drosophila trachea. Development **129:**4941–4951.
7. **Franch-Marro, X., and J. Casanova.** 2002. spalt-induced specification of distinct dorsal and ventral domains is required for Drosophila tracheal patterning. Dev. Biol. **250:**374–382.
8. **Ghabrial, A., S. Luschnig, M. M. Metzstein, and M. A. Krasnow.** 2003. Branching morphogenesis of the Drosophila tracheal system. Annu. Rev. Cell Dev. Biol. **19:**623–647.
9. **Ikeya, T., and S. Hayashi.** 1999. Interplay of Notch and FGF signaling restricts cell fate and MAPK activation in the Drosophila trachea. Development **126:**4455–4463.
10. **Isaac, D. D., and D. J. Andrew.** 1996. Tubulogenesis in *Drosophila*: a requirement for the *trachealess* gene product. Genes Dev. **10:**103–117.
11. **Jazwinska, A., and M. Affolter.** 2004. A family of genes encoding zona pellucida (ZP) domain proteins is expressed in various epithelial tissues during Drosophila embryogenesis. Gene Expr. Patterns **4:**413–421.
12. **Jiang, L., and S. T. Crews.** 2003. The Drosophila dysfusion basic helix-loop-helix (bHLH)-PAS gene controls tracheal fusion and levels of the trachealess bHLH-PAS protein. Mol. Cell. Biol. **23:**5625–5637.
13. **Kearney, J. B., S. R. Wheeler, P. Estes, B. Parente, and S. T. Crews.** 2004. Gene expression profiling of the developing Drosophila CNS midline cells. Dev. Biol. **275:**473–492.
14. **Klambt, C., L. Glazer, and B.-Z. Shilo.** 1992. *breathless*, a Drosophila FGF receptor homolog, is essential for migration of tracheal and specific midline glial cells. Genes Dev. **6:**1668–1678.
15. **Kuhnlein, R. P., and R. Schuh.** 1996. Dual function of the region-specific homeotic gene spalt during Drosophila tracheal system development. Development **122:**2215–2223.
16. **Lavista-Llanos, S., L. Centanin, M. Irisarri, D. M. Russo, J. M. Gleadle, S. N. Bocca, M. Muzzopappa, P. J. Ratcliffe, and P. Wappner.** 2002. Control of the hypoxic response in *Drosophila melanogaster* by the basic helix-loop-helix PAS protein similar. Mol. Cell. Biol. **22:**6842–6853.
17. **Moser, M., R. Knoth, C. Bode, and C. Patterson.** 2004. LE-PAS, a novel Arnt-dependent HLH-PAS protein, is expressed in limbic tissues and transactivates the CNS midline enhancer element. Brain Res. Mol. Brain Res. **128:**141–149.
18. **Myat, M. M., H. Lightfoot, P. Wang, and D. J. Andrew.** 2005. A molecular link between FGF and Dpp signaling in branch-specific migration of the Drosophila trachea. Dev. Biol. **281:**38–52.
19. **Nambu, J. R., W. Chen, S. Hu, and S. T. Crews.** 1996. The *Drosophila melanogaster similar bHLH-PAS* gene encodes a protein related to human hypoxia-inducible factor 1α and *Drosophila* Single-minded. Gene **172:**249–254.
20. **Ohshiro, T., and K. Saigo.** 1997. Transcriptional regulation of *breathless* FGF receptor gene by binding of TRACHEALESS/dARNT heterodimers to three central midline elements in *Drosophila* developing trachea. Development **124:**3975–3986.
21. **Ooe, N., K. Saito, N. Mikami, I. Nakatuka, and H. Kaneko.** 2004. Identification of a novel basic helix-loop-helix-PAS factor, NXF, reveals a Sim2 competitive, positive regulatory role in dendritic-cytoskeleton modulator drebrin gene expression. Mol. Cell. Biol. **24:**608–616.
22. **Patel, N. H., P. M. Snow, and C. S. Goodman.** 1987. Characterization and cloning of fasciclin III: a glycoprotein expressed on a subset of neurons and axon pathways in Drosophila. Cell **48:**975–988.
23. **Powell-Coffman, J. A.** 2003. bHLH-PAS proteins in *C. elegans*, p. 51–68. *In* S. T. Crews (ed.), PAS proteins: regulators and sensors of development and physiology. Kluwer Academic Publishers, Dordrecht, The Netherlands.
24. **Ribeiro, C., A. Ebner, and M. Affolter.** 2002. In vivo imaging reveals different cellular functions for FGF and Dpp signaling in tracheal branching morphogenesis. Dev. Cell **2:**677–683.
25. **Roth, P., N. Xylourgidis, N. Sabri, A. Uv, M. Fornerod, and C. Samakovlis.** 2003. The Drosophila nucleoporin DNup88 localizes DNup214 and CRM1 on the nuclear envelope and attenuates NES-mediated nuclear export. J. Cell Biol. **163:**701–706.
26. **Samakovlis, C., N. Hacohen, G. Manning, D. Sutherland, K. Guillemin, and M. A. Krasnow.** 1996. Development of the Drosophila tracheal system occurs by a series of morphologically distinct but genetically coupled branching events. Development **122:**1395–1407.
27. **Samakovlis, C., G. Manning, P. Steneberg, N. Hacohen, R. Cantera, and M. A. Krasnow.** 1996. Genetic control of epithelial tube fusion during Drosophila tracheal development. Development **122:**3531–3536.
28. **Sato, M., and T. B. Kornberg.** 2002. FGF is an essential mitogen and chemoattractant for the air sacs of the Drosophila tracheal system. Dev. Cell **3:**195–207.
29. **Sonnenfeld, M., M. Ward, G. Nystrom, J. Mosher, S. Stahl, and S. Crews.** 1997. The *Drosophila tango* gene encodes a bHLH-PAS protein that is orthologous to mammalian Arnt and controls CNS midline and tracheal development. Development **124:**4583–4594.
30. **Sutherland, D., C. Samakovlis, and M. A. Krasnow.** 1996. *branchless* encodes a Drosophila FGF homolog that controls tracheal cell migration and the pattern of branching. Cell **87:**1091–1101.
31. **Tanaka-Matakatsu, M., T. Uemura, H. Oda, M. Takeichi, and S. Hayashi.** 1996. Cadherin-mediated cell adhesion and cell motility in Drosophila trachea regulated by the transcription factor Escargot. Development **122:**3697–3705.
32. **Tomancak, P., A. Beaton, R. Weiszmann, E. Kwan, S. Shu, S. E. Lewis, S. Richards, M. Ashburner, V. Hartenstein, S. E. Celniker, et al.** 2002. Systematic determination of patterns of gene expression during Drosophila embryogenesis. Genome Biol. **3:**RESEARCH0088.
33. **Uemura, T., H. Oda, R. Kraut, S. Hayashi, Y. Kotaoka, and M. Takeichi.** 1996. Zygotic Drosophila E-cadherin expression is required for processes of dynamic epithelial cell rearrangement in the Drosophila embryo. Genes Dev. **10:**659–671.
34. **Uv, A., R. Cantera, and C. Samakovlis.** 2003. Drosophila tracheal morphogenesis: intricate cellular solutions to basic plumbing problems. Trends Cell Biol. **13:**301–309.
35. **Uv, A. E., P. Roth, N. Xylourgidis, A. Wickberg, R. Cantera, and C. Samakovlis.** 2000. members only encodes a Drosophila nucleoporin required for rel protein import and immune response activation. Genes Dev. **14:**1945–1957.
36. **Ward, M. P., J. T. Mosher, and S. T. Crews.** 1998. Regulation of *Drosophila* bHLH-PAS protein cellular localization during embryogenesis. Development **125:**1599–1608.
37. **Wilk, R., I. Weizman, L. Glazer, and B.-Z. Shilo.** 1996. *trachealess* encodes a bHLH-PAS protein and is a master regulator gene in the *Drosophila* tracheal system. Genes Dev. **10:**93–102.